

## On the limits of spin-exchange optical pumping of $^3\text{He}$

W. C. Chen, T. R. Gentile, Q. Ye, T. G. Walker, and E. Babcock

Citation: *Journal of Applied Physics* **116**, 014903 (2014); doi: 10.1063/1.4886583

View online: <http://dx.doi.org/10.1063/1.4886583>

View Table of Contents: <http://scitation.aip.org/content/aip/journal/jap/116/1?ver=pdfcov>

Published by the [AIP Publishing](#)

---

### Articles you may be interested in

[Development of a compact in situ polarized  \$^3\text{He}\$  neutron spin filter at Oak Ridge National Laboratory](#)

*Rev. Sci. Instrum.* **85**, 075112 (2014); 10.1063/1.4890391

[Measurement of laser heating in spin exchange optical pumping by NMR diffusion sensitization gradients](#)

*J. Appl. Phys.* **107**, 094904 (2010); 10.1063/1.3371249

[He 3 polarization via optical pumping in a birefringent cell](#)

*Appl. Phys. Lett.* **87**, 053506 (2005); 10.1063/1.2008370

[Spin-exchange optically pumped polarized He 3 target for low-energy charged particle scattering experiments](#)

*Rev. Sci. Instrum.* **76**, 033503 (2005); 10.1063/1.1866235

[Spin-exchange optical pumping of high-density xenon-129](#)

*J. Chem. Phys.* **118**, 1581 (2003); 10.1063/1.1539042

---



## On the limits of spin-exchange optical pumping of $^3\text{He}$

W. C. Chen,<sup>1,2,a)</sup> T. R. Gentile,<sup>2</sup> Q. Ye,<sup>1,2</sup> T. G. Walker,<sup>3</sup> and E. Babcock<sup>4</sup>

<sup>1</sup>University of Maryland, College Park, Maryland 20742, USA

<sup>2</sup>National Institute of Standards and Technology (NIST), Gaithersburg, Maryland 20899, USA

<sup>3</sup>University of Wisconsin, Madison, Wisconsin 53706, USA

<sup>4</sup>Juelich Centre for Neutron Science at FRM 2, Forschungszentrum Juelich GmbH, 85747 Garching, Germany

(Received 11 April 2014; accepted 21 June 2014; published online 2 July 2014)

We have obtained improvement in the  $^3\text{He}$  polarization achievable by spin-exchange optical pumping (SEOP). These results were primarily obtained in large neutron spin filter cells using diode bar lasers spectrally narrowed with chirped volume holographic gratings. As compared to our past results with lasers narrowed with diffraction gratings, we have observed between 5% and 11% fractional increase in the  $^3\text{He}$  polarization  $P_{\text{He}}$ . We also report a comparable improvement in  $P_{\text{He}}$  for two small cells, for which we would not have expected an increase from improved laser performance. In particular, prior extensive studies had indicated that the alkali-metal polarization was within 3% of unity in one of these cells. These results have impact on understanding the maximum  $P_{\text{He}}$  achievable by SEOP, whether the origin of the improvement is from increased alkali-metal polarization or decreased temperature-dependent relaxation. We conclude that the most likely explanation for the improvement in  $P_{\text{He}}$  is increased alkali-metal polarization. We have observed  $P_{\text{He}}$  of between 0.80 and 0.85 in several large cells, which marks a new precedent for the polarization achievable by SEOP. © 2014 AIP Publishing LLC. [<http://dx.doi.org/10.1063/1.4886583>]

### I. INTRODUCTION

Spin-exchange optical pumping (SEOP) of  $^3\text{He}$  has widespread application for neutron spin filters,<sup>1–6</sup> polarized targets,<sup>7,8</sup> and medical imaging.<sup>9</sup> About a decade ago, improved measurements of the spin-exchange rate coefficient<sup>10</sup> revealed a linear increase in the  $^3\text{He}$  wall relaxation rate with alkali-metal density for SEOP cells under operating conditions. Several improvements in the methods and diagnostics for SEOP allowed for a detailed study of the polarization limits set by this relaxation phenomenon.<sup>11</sup> These improvements include cells with relaxation times of hundreds of hours;<sup>12</sup> optical pumping with spectrally narrowed diode laser arrays;<sup>13</sup> alkali-metal polarization measurements;<sup>10</sup> and accurate  $^3\text{He}$  polarization measurements by neutron transmission<sup>14</sup> and electron paramagnetic resonance (EPR).<sup>15,16</sup> In general, the limitation was quantified by the parameter  $X$  that is proportional to the slope of the  $^3\text{He}$  wall relaxation rate with alkali-metal density

$$P_{\text{He}} = P_{\text{Rb}} \frac{k_{\text{se}}[\text{Rb}]}{k_{\text{se}}[\text{Rb}](1 + X) + \Gamma_r}. \quad (1)$$

Here,  $P_{\text{He}}$  and  $P_{\text{Rb}}$  are the  $^3\text{He}$  and rubidium polarizations, respectively,  $k_{\text{se}}$  is the spin-exchange rate coefficient,  $[\text{Rb}]$  is the Rb density, and  $\Gamma_r$  is the room temperature  $^3\text{He}$  relaxation rate. The  $^3\text{He}$  polarization asymptotically approaches its maximum value  $P_{\text{He}}$  with an exponential time constant  $T_{\text{up}} = \{k_{\text{se}}[\text{Rb}](1 + X) + \Gamma_r\}^{-1}$ . Equation (1) can be generalized for Rb/K mixture cells.<sup>10</sup>

The most extensive group of cells in which the highest polarization values have been reached are neutron spin filter

cells, which are typically large, cylindrical, blown GE180 (Ref. 17) glass cells with relaxation times of 150 h or longer.<sup>1,18,19</sup> Until this work, the maximum achievable  $P_{\text{He}}$  in such cells was between 0.75 and 0.80, for cells with  $X \approx 0.25$ . (Assuming that the only limit to  $P_{\text{He}}$  were from anisotropic spin-exchange, the maximum achievable value of  $P_{\text{He}}$  is expected to be 0.96.<sup>20,21</sup>) Based on the conclusions of Ref. 10, it was expected that further improvements in laser technology might improve the  $^3\text{He}$  polarizing rate, but that the achievable  $^3\text{He}$  polarization was limited by the temperature dependence of the  $^3\text{He}$  wall relaxation rate. (This statement applies to cells for which  $k_{\text{se}}[\text{Rb}] \gg \Gamma_r$ , for which faster spin-exchange has only a small effect on maximum polarization.) Here, we report that conversion of our optical feedback scheme for spectral narrowing from a diffraction grating to a chirped volume holographic grating (VHG) has surprisingly yielded between 5% and 11% fractional improvement in the achievable  $^3\text{He}$  polarization in large cells. Cell to cell variations in  $X$  still determine the achievable polarization but overall the polarization values are higher, which indicate that our  $X$  values are smaller than previously evaluated.

The key question which we consider but cannot definitively answer is whether the increase in  $^3\text{He}$  polarization observed is simply due to increased alkali-metal polarization. We do not report direct measurements of alkali-metal polarization, but do reference past measurements on one of the cells studied. We first observed these results in large, blown cells, for which a possible improvement in volume-averaged alkali-metal polarization might have been expected. Our past studies of such cells used indirect determinations of alkali-metal polarization, with the assumption of a maximum value of unity.<sup>10,22</sup> Hence, we tested the achievable polarization in small cells, in particular a flat-windowed cell for which in prior studies<sup>10</sup> the achievable volume-averaged alkali-metal

<sup>a)</sup>Electronic address: wchen@nist.gov

polarization had been carefully determined by direct measurements to be within 3% of unity. We observed some increase in polarization in small cells, suggesting that the alkali-metal polarizations deduced in the previous work were systematically high.

Our results have yielded practical value for neutron spin filters.<sup>23,24</sup> Improved  $^3\text{He}$  polarization is important for all applications of polarized  $^3\text{He}$  but is particularly relevant to neutron spin filters. In a typical nuclear physics experiment, the running time for a given statistical uncertainty is inversely proportional to  $P_{\text{He}}^2$ , which is the relevant figure of merit for measurement of a small asymmetry proportional to the  $^3\text{He}$  polarization. However, in many polarization analysis experiments in neutron scattering a small component of magnetic scattering is to be separated from a strong background of nuclear scattering.<sup>25</sup> In this case, it can be shown that the running time varies roughly as  $P_{\text{He}}^4$  for the current typical range of achievable polarization. Hence, a 10% increase in  $^3\text{He}$  polarization can yield nearly a 50% decrease in running time for these demanding experiments.

VHGs contain planes of varying index of refraction fabricated in photorefractive glass,<sup>26,27</sup> that produce a wavelength-selective reflection. VHG-based fiber-coupled diode laser arrays have been applied to SEOP of xenon<sup>28</sup> and polarized  $^3\text{He}$  targets.<sup>8,29</sup> In a chirped VHG, the selected wavelength varies across the VHG optic, which is convenient and flexible for spectral narrowing of free space lasers.

Here, we focus on studies to understand the ramifications and origin of the observed improvements in achievable  $^3\text{He}$  polarization. In Sec. II, we briefly describe the salient features of our apparatus relevant for these studies. We present our results for polarization improvement in Sec. III, and discuss the ramifications for SEOP in Sec. IV. We consider possible differences between the laser configurations in Sec. V. We summarize our conclusions in Sec. VI.

## II. APPARATUS

The apparatus and laser systems we employ have been described elsewhere.<sup>1</sup> Currently, in each system we employ two lasers, each based on a 100 W diode bar.<sup>30</sup> A diagram of the optical system for the chirped VHG configuration is shown in Fig. 1. In most cases, we optically pump blown cylindrical cells through the curved sides of the cell to avoid the focusing

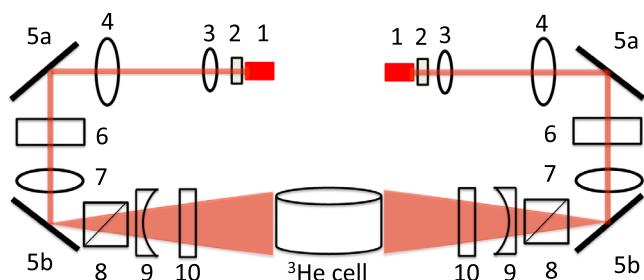


FIG. 1. Diagram of the optical system for the chirped VHG configuration, showing the diode laser array (1), chirped VHG (2), telescope lenses (3, 4), steering mirrors (5a, 5b), cylindrical lens (6), spherical lens (7), polarizing beamsplitter cube for a horizontally polarized laser (8), diverging cylindrical lens (used when needed for long cells) (9), quarter-wave plate (10), and a side-pumped  $^3\text{He}$  cell.

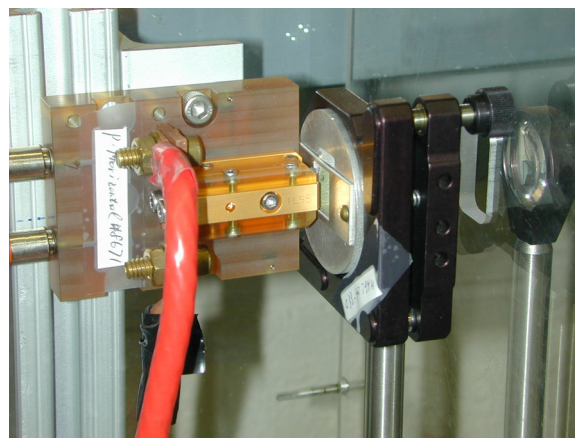


FIG. 2. A chirped volume holographic grating mounted in front of a 100 W diode laser bar.

of laser light that occurs when transmitting light through the non-uniform ends. To avoid possible dark areas in the cell, we send laser light through opposite sides of the cell.

For the diffraction grating configuration, we employed a polarizing beam splitter cube instead of the first steering mirror (labelled 5a in Fig. 1) and a half-wave plate between the telescope lenses (3, 4 in Fig. 1) to control the feedback to the laser.<sup>31</sup> The main beam was reflected by the beamsplitter cube while a weaker beam was transmitted to the diffraction grating. The optic axis of the half-wave plate was typically adjusted to rotate the linear polarization of the laser light by between  $25^\circ$  and  $30^\circ$  relative to the minimum feedback condition.

The VHGs<sup>32</sup> are 14 mm tall (dimension along the 10 mm bar length), 14 mm wide, and 1.75 mm thick, with a “chirp” of 0.15 nm/mm in the feedback wavelength along the width. Tuning of the laser is accomplished by simply translating the VHG across the laser beam. As shown in Fig. 2, the VHG is held in a mount that allows for rotation of the grating, and horizontal and vertical angular adjustment to maximize the efficiency of feedback and thus yield the highest power with the minimum amount of residual light in the typical 2 nm FWHM (full width at half maximum) free-running spectrum. A typical spectrum is shown in Fig. 3. The central wavelength of the chirped VHG was specified to be 0.9 nm below the actual Rb transition wavelength due to the typical observed central wavelength shift from optical heating of the VHG. Since the temperature rise will vary for different grating properties, the mounting arrangement, the laser power, etc., the desired wavelength specification will also vary.

Values of the  $^3\text{He}$  polarization  $P_{\text{He}}$  were determined with a typical relative standard uncertainty of 3% by adiabatic fast passage nuclear magnetic resonance (NMR) measurements that were calibrated against neutron transmission. The relative precision in  $P_{\text{He}}$ , which is relevant to comparing  $^3\text{He}$  polarization results for the different laser configurations for a given cell, is typically 1.5%. Neutron transmission measurements were performed on several monochromatic beam lines at the NIST Center for Neutron Research. Past reported results<sup>10,22</sup> primarily employed the NG6M cold neutron beam line.<sup>33</sup> More recent results for large spin filter



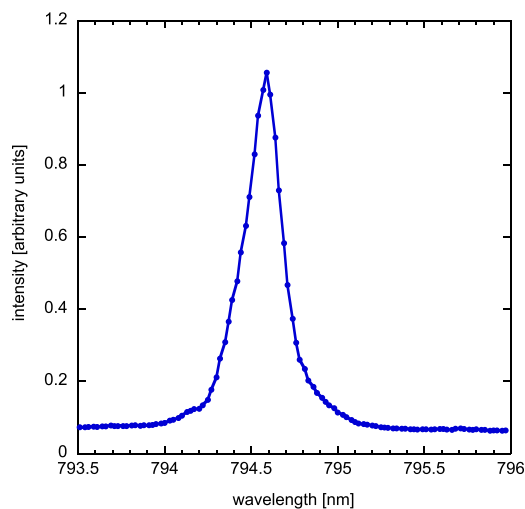


FIG. 3. Typical spectrum for a 100 W diode bar operated at 95 A (output power of 80 W) and spectrally narrowed with a chirped VH. The data were obtained with a spectrum analyzer with a resolution of 0.05 nm. The baseline level is from instrumental background. The full width at half maximum is 0.25 nm.

cells routinely used for neutron scattering experiments were obtained on the Advanced Neutron Diffractometer/Reflectometer (AND/R),<sup>34</sup> BT7 thermal triple-axis spectrometer,<sup>35</sup> the quasi-monochromatic NG3 SANS (small angle neutron scattering spectrometer),<sup>36</sup> and the new NG6A cold neutron beam line. The polarization values listed were either based on neutron transmission measurements immediately after transporting the polarized cell to a neutron beam line, or based on an adiabatic fast passage NMR signal that was calibrated against such a neutron test. Whereas in our past studies,<sup>10,12</sup> we applied a 2% correction for loss of polarization due to transport to the neutron beam line, we no longer apply this correction because tests with improved transport indicate essentially no loss.

### III. RESULTS

Table I documents our results with large, Rb/K hybrid<sup>22,37</sup> spin filter cells. The results with the chirped VH scheme have been primarily obtained after 2010, whereas the diffraction grating results were obtained between 2007 and 2010. For the older cells Syrah and Chardonnay, these

TABLE I. Comparison of achievable <sup>3</sup>He polarization in large, Rb/K hybrid cells with lasers spectrally narrowed with chirped VHs or diffraction gratings. Listed parameters are the vapor mixture ratio at operating temperature,  $D = [K]/[Rb]$ ; cell volume  $V$  in  $\text{cm}^3$ ; cell relaxation time  $T_1$  (Ref. 38) in hours; pumping time constant  $T_{\text{up}}$  in hours for tests with VH lasers; polarization for optical pumping with chirped VH-based lasers  $P_{\text{He}}^{\text{VHG}}$ ; and polarization for optical pumping with diffraction grating-based lasers  $P_{\text{He}}^{\text{DG}}$ .

Cell	$D$	$V$ ( $\text{cm}^3$ )	$T_1$ (h)	$T_{\text{up}}$ (h)	$P_{\text{He}}^{\text{VHG}}$	$P_{\text{He}}^{\text{DG}}$
Burgundy	4.0	900	203	4.8, 8	0.85	0.78
Maverick	4	620	208	4.3, 8.9	0.82	0.77
Syrah	6.2	790	450	4.0	0.83	0.77
Chablis	7	950	190	4.3	0.77	0.72
Olaf	4.4	550	350	4.5	0.80	0.72
Chardonnay	1.6	400	390	6, 8	0.84	0.77

diffraction grating results agree with those documented in prior studies.<sup>22</sup> The improvement in achievable polarization varies between 5% and 11% for the cells listed. For the chirped VH tests, the total laser power incident on the SEOP oven was typically 110 W, whereas for the diffraction grating results this value was typically 90 W. In both cases, the diode bars were operated at reduced current (95 A, yielding an output power of 80 W) because of the increased intensity at the diode bar due to the optical feedback. However, the simple increase in laser power is not the sole origin of the improvement; a test for the cell Burgundy with 90 W from the chirped VH lasers yielded less than a 2% fractional decrease from the maximum polarization. In addition, past studies performed with only 52 W of laser power indicated that the alkali-metal polarization was saturated and assumed to be within 5% of unity<sup>10,22</sup> and the increase in laser power to 90 W (before the conversion to chirped VHs) had not resulted in improved polarization.

The reported values of <sup>3</sup>He polarization are based on unpolarized neutron transmission measurements. Measurements with highly polarized neutron beams, while not needed, provided an additional check on the observed increases. The quality of a polarized neutron beam apparatus consisting of a polarizer, spin flipper, and analyzer is typically characterized by the flipping ratio  $F = T_+/T_-$ , where  $T_+$  and  $T_-$  are the transmissions for the spin flipper off and on, respectively.<sup>39</sup> The AND/R reflectometer is equipped with a supermirror polarizer (polarizing efficiency of  $0.991 \pm 0.001$ ) and a precession coil spin flipper (efficiency of  $0.999 \pm 0.001$ ); for the spin filter cell Burgundy the typical flipping ratio increased from 70 to 95 (precision for  $F$  is  $\pm 2$ ), consistent with an increase in  $P_{\text{He}}$  from 0.77 to 0.85.

In prior studies, the alkali-metal polarization in these large cells was found to increase as the temperature (and thus the alkali-metal spin relaxation rate) was decreased, and saturated at a maximum value at low cell temperatures. The maximum value observed was presumed to be unity.<sup>22</sup> However, if light does not reach some part of the cell due to distortion of the laser beam and/or spatial inhomogeneity of the laser beam, the alkali-metal polarization may saturate but not necessarily be unity throughout the entire cell. Hence, we pursued additional tests on two small cells, denoted Wilma and Betty. The cell Betty has flat, optically sealed end windows and prior extensive tests indicated that the alkali-metal polarization was within 3% of unity at all points within the cell.<sup>10</sup> For such small cells, we did not expect any improvement in the <sup>3</sup>He polarization. Nevertheless, we did observe some increase in polarization: for the cells Wilma and Betty, we obtained  $P_{\text{He}} = 0.79$  and  $P_{\text{He}} = 0.78$ , as compared to our previously documented values of 0.76 and 0.72, respectively.<sup>10,12</sup>

### IV. RAMIFICATIONS FOR SEOP

Our results suggest that the volume-averaged alkali-metal polarization for SEOP with our diffraction grating lasers was lower than unity. Recently, it was found that the transverse EPR method for measuring alkali-metal polarization yielded lower values than the longitudinal method

previously employed.<sup>40</sup> However, this discrepancy was found to decrease with increasing alkali-metal polarization; in the regime in which the longitudinal method yielded alkali-metal polarization close to unity, the methods differed by less than 2%. Hence, this small discrepancy between transverse and longitudinal EPR is insufficient to explain our results. A possible issue in alkali-metal polarization measurements is the validity of assuming that a true line average along the probe laser beam is being sampled. If not, the contributions of regions with alkali-metal polarization less than unity might be undersampled.

For the small, flat-windowed cell Betty, further tests led to the surprising result that most of the observed improvement could also be obtained with diffraction grating lasers. Even upon decreasing the laser power for a single diffraction grating laser to 14 W as was used in the previous reports,<sup>10,12</sup> we still obtained  $P_{\text{He}} = 0.75$ . In contrast with most of our cells which have been tested over the years with increasing laser power,<sup>1</sup> the cell Betty had not been tested for nearly a decade. The origin of the difference between  $P_{\text{He}} = 0.75$  obtained now as compared to the earlier result of  $P_{\text{He}} = 0.72$  for nominally the same conditions was not investigated and presumed to be due to some combination of uncertainties in the measurements and, given the long intervening time period, changes in the optical pumping conditions. Nevertheless, when the value of 0.72 was obtained, extensive tests to establish that the alkali-metal polarization was within 3% of unity were reported. Therefore, all of our data suggest that we have obtained a small gain in alkali-metal polarization that was primarily revealed by the use of chirped VHG lasers but in some cases is also related to increased laser power. The maximum polarization of 0.78 in the cell Betty was obtained with either 50 W of laser power incident from one side of the cell or with 50 W incident from each side (total of 100 W).

In Ref. 10, determinations of  $X$  from measurements of hot relaxation were reported and generally agreed within uncertainties with  $X$  values based on maximum achievable  $P_{\text{He}}$ . However, both of these methods would yield lower values of  $X$  if the alkali-polarization were less than unity. As discussed in Ref. 13, Faraday rotation is proportional to the product of alkali-metal density and alkali-metal polarization, thus if the alkali-metal polarization were overestimated, the alkali-metal density would have been underestimated and thus  $X$  would have been overestimated. Independent determinations of the alkali-metal density not reliant on knowledge of the alkali-metal polarization were reported in Ref. 13 and all approaches agreed within 15%. Therefore, the relatively small decrease in alkali-metal polarization suggested by our current results is not inconsistent with the uncertainties in Ref. 13.

An alternative, more exotic explanation for our results is that higher spectral power density at the Rb resonance is actually affecting  $X$ , as the origin of temperature-dependent relaxation is not understood. In Ref. 10, it was speculated that the excess relaxation could be associated with the alkali-metal film itself, which perhaps could be affected by stronger absorption by the Rb on the surface of the cell. However, in past studies<sup>41</sup> on the small, flat-windowed cell Betty, measurements of  $X$  were found to be independent of whether a

spectrally narrowed or broadband laser was employed for the optical pumping, and independent of whether the relaxation time was determined from the optical pumping time constant or from hot relaxation with the laser off. Hence it seems unlikely that the relaxation properties of the cell are different for the VHG narrowing scheme. However, one expects the best values of  $X$  for the low surface to volume ratios for large cells.<sup>10</sup> It appears that those values were underestimated in the past, perhaps due to the high demands such cells present for reaching 100% volume-averaged alkali-metal polarization.

In Ref. 22, determinations of the decrease in alkali-metal polarization with increasing spin-exchange rate were compared to a basic model for SEOP. The alkali-metal polarization was determined indirectly from measurement of  $P_{\text{He}}$  and other parameters rather than by direct measurements. The calculations were performed by modelling the absorption of laser light in the cell and the resultant position-dependent alkali-metal polarization, and included a loss term for absorption of unpolarized alkali-metal on the cell walls. Typically, the experimental results showed a faster decrease with increasing spin-exchange rate than the models, in particular for pure Rb cells. However, at sufficiently slow spin-exchange rates, both the models and direct alkali-metal polarization measurements indicated the saturated value of the alkali-metal polarization was within 3% of unity. Using this model, we performed calculations for the optical pumping conditions studied in this work and also find that even for the demanding cell Burgundy the alkali-metal polarization should be within 3% of unity. A number of new effects that will decrease the calculated alkali-metal polarization have recently been reported, including circular dichroism,<sup>42</sup> potassium absorption,<sup>43</sup> excited state relaxation, radiation trapping, and laser heating.<sup>44</sup> Work is in progress to develop a complete model that will include all these effects. It is likely that such an improved model will affect the comparison to measured results, but primarily for large cells optically pumped at relatively high spin-exchange rates rather than small cells or low rates.

## V. DISCUSSION OF LASERS

The ramifications discussed above apply regardless of whether VHG-narrowed lasers are required to obtain the improvements we have obtained. Nevertheless, for large cells, we only observed the improvement with VHG-narrowed lasers, hence we attempted to test whether there is some simple difference between laser properties for the chirped VHG narrowing scheme as compared to the diffraction grating scheme. Although the VHG narrowing scheme yields more power because of the absence of the conventional diffraction grating, our tests above indicate that this is not the only parameter. Both lasers yield comparable spectral linewidths ranging between 0.2 nm and 0.3 nm depending on diode bar quality and operating current. However, we find that the jitter in the spectrally narrowed peak is small compared to the linewidth for the chirped VHG scheme, whereas the jitter for the diffraction grating scheme may increase the effective linewidth by  $\approx 0.1$  nm.

On the average, the VHG-narrowed system has a lower level of residual broadband light. Such light is undesirable

not just because it reduces the spectral power density, but also because it results in lower maximum alkali-metal polarization.<sup>42</sup> This may be the most notable feature of the chirped VHG scheme. However, when the VHG-narrowed lasers were misaligned to produce a level of background similar to that observed for the diffraction grating scheme, the resulting decline in <sup>3</sup>He polarization for the cell Chardonnay was  $\leq 1\%$ . For the conditions of this test, our modelling also predicted  $\leq 1\%$  decrease in alkali-metal polarization.

One possibility for the different performance of the two types of narrowing is the spatial structure of the laser beam, although the lenses used for both schemes were identical. In addition, for 100 W lasers we use a diffraction grating scheme in which the grating only provides feedback and is not in the beam that is used to illuminate the cell. Hence, spatial structure seems to be an unlikely origin.

The chirped VHG lasers were found to allow for faster optical pumping, hence most of the results in Table I were obtained with fairly short pumping time constants  $T_{up}$  between 4 h and 5 h, shorter than the typical values of between 7 h and 8 h for SEOP with the diffraction grating lasers. It is interesting how the change in our operational pumping time constants arose. We measure the cell temperature with a thermal sensor located on or near contact with the cell. We find that the true temperature of the alkali-metal, as determined from the observed pumping time constant for a known value of  $X$ , can be higher than the sensor temperature. However, for large cells, the observed temperature elevation is typically less than 10 °C. Upon first switching from diffraction gratings to chirped VHGs, we found that the time constants for pumping large cells typically shortened by a factor that implied an additional temperature increase of  $\approx 10$  °C. We attribute this elevation to increased spectral laser power density for spectral narrowing with the chirped VHG system, due to higher overall power and better suppression of broadband emission. Since the <sup>3</sup>He polarizations also increased, we continued operation with the shorter time constants. Because of the long room temperature relaxation times for the cells employed, the expected fractional increase in <sup>3</sup>He polarization from simple rate balance (Eq. (1)) is less than 2%. In principle, this expected fractional increase could vary if the excess relaxation were not linear with alkali-metal density as in Eq. (1). However, the tests with longer time constants indicated in Table I also yielded essentially the same polarization. In addition, the tests on small cells were performed with comparable cell temperature for both the VHG and diffraction grating lasers.

## VI. CONCLUSION

In conclusion, we have observed a fractional increase of between 5% and 11% in the achievable <sup>3</sup>He polarization in large SEOP cells using chirped VHG-narrowing of diode bar lasers as compared to diffraction-grating narrowing. The maximum polarization we have observed is  $P_{He} = 0.85$  in a neutron spin filter cell nearly 1 l in volume. We believe that the most likely explanation for these results is increased volume-averaged alkali-metal polarization, despite past studies that indicated that within 3% of unity had already been

reached with lasers employing the diffraction grating scheme. This suggests that EPR-based measurements systematically overestimate alkali-metal polarizations. We have not clearly identified a particular feature of the VHG narrowing scheme that explains our results. Nevertheless, it is likely that the higher spectral power density, lower broadband background, and better wavelength stability have yielded increased alkali-metal polarization.

If indeed the improved performance of the VHG lasers is due to superior spectral qualities, it raises the question as to whether additional improvements can be realized. Whereas in the past  $P_{He}$  up to 0.79 was reported for SEOP with ultra-narrow Ti-sapphire lasers,<sup>45</sup> current applications rely almost entirely on diode lasers due to greater economy, simplicity and available power. It is possible that SEOP with either ultra-narrow high power diode laser systems<sup>32</sup> or with high-power alkali-metal lasers<sup>46</sup> could yield further improvements in <sup>3</sup>He polarization.

## ACKNOWLEDGMENTS

We thank S. Watson, B. Maranville, R. W. Erwin, and M. G. Huber for assistance with neutron measurements, and J. A. Anderson and J. Fuller for fabrication of the <sup>3</sup>He cells. The development and application of neutron spin filters has been supported in part by the U.S. Department of Energy, Basic Energy Sciences. The work utilized facilities supported in part by the National Science Foundation under Agreement No. DMR-0944772.

<sup>1</sup>W. C. Chen *et al.*, *J. Phys.: Conf. Ser.* **294**, 012003 (2011), and references therein.

<sup>2</sup>E. Babcock, Z. Salhi, M-S. Appavou, A. Feoktystov, V. Pipich, A. Radulescu, V. Ossovyi, S. Staringer, and A. Ioffe, *Phys. Procedia* **42**, 154 (2013).

<sup>3</sup>C. J. Beecham, S. Boag, C. D. Frost, T. J. McKetterick, J. R. Stewart, K. H. Andersen, P. M. Bentley, and D. Jullien, *Physica B* **406**, 2429 (2011).

<sup>4</sup>C. Y. Jiang *et al.*, *Phys. Procedia* **42**, 191 (2013).

<sup>5</sup>H. Kira *et al.*, *J. Phys.: Conf. Ser.* **294**, 012014 (2011).

<sup>6</sup>Y. Sakaguchi *et al.*, *J. Phys.: Conf. Ser.* **294**, 012017 (2011).

<sup>7</sup>P. A. M. Dolph, J. Singh, T. Averett, A. Kelleher, K. E. Mooney, V. Nelyubin, W. A. Tobias, B. Wojtsekhowski, and G. D. Cates, *Phys. Rev. C* **84**, 065201 (2011).

<sup>8</sup>Q. Ye, G. Laskaris, W. Chen, H. Gao, W. Zheng, X. Zong, T. Averett, G. D. Cates, and W. A. Tobias, *Eur. Phys. J. A* **44**, 55 (2010).

<sup>9</sup>E. J. R. van Beek *et al.*, *J. Magn. Reson. Imaging* **20**, 540 (2004); M. S. Albert *et al.*, *Nature* **370**, 199 (1994).

<sup>10</sup>B. Chann, E. Babcock, L. W. Anderson, and T. G. Walker, *Phys. Rev. A* **66**, 032703 (2002).

<sup>11</sup>E. Babcock, B. Chann, T. G. Walker, W. C. Chen, and T. R. Gentile, *Phys. Rev. Lett.* **96**, 083003 (2006).

<sup>12</sup>D. R. Rich, T. R. Gentile, T. B. Smith, A. K. Thompson, and G. L. Jones, *Appl. Phys. Lett.* **80**, 2210 (2002).

<sup>13</sup>B. Chann *et al.*, *J. Appl. Phys.* **94**, 6908 (2003).

<sup>14</sup>G. L. Jones *et al.*, *Nucl. Instrum. Methods Phys. Res. A* **440**, 772 (2000).

<sup>15</sup>E. Babcock, I. A. Nelson, S. Kadlecck, and T. G. Walker, *Phys. Rev. A* **71**, 013414 (2005);

<sup>16</sup>M. V. Romalis and G. D. Cates, *Phys. Rev. A* **58**, 3004 (1998).

<sup>17</sup>GE Lighting Component Sales, Bldg. 315D, 1975 Noble Rd., Cleveland, OH 44117. Certain trade names and company products are mentioned in the text or identified in an illustration in order to adequately specify the experimental procedure and equipment used. In no case does such identification imply recommendation or endorsement by the National Institute of Standards and Technology, nor does it imply that the products are necessarily the best available for the purpose.

<sup>18</sup>E. Babcock, S. Mattauch, and A. Ioffe, *Nucl. Instrum. Methods Phys. Res. A* **625**, 43 (2011).

<sup>19</sup>S. R. Parnell *et al.*, *Nucl. Instrum. Methods Phys. Res. A* **598**, 774 (2009).

- <sup>20</sup>T. V. Tscherbul, P. Zhang, H. R. Sadeghpour, and A. Dalgarno, *Phys. Rev. Lett.* **107**, 023204 (2011).
- <sup>21</sup>D. K. Walter, W. Happer, and T. G. Walker, *Phys. Rev. A* **58**, 3642 (1998).
- <sup>22</sup>W. C. Chen, T. R. Gentile, T. G. Walker, and E. Babcock, *Phys. Rev. A* **75**, 013416 (2007).
- <sup>23</sup>Information about the neutron spin filter program at NIST can be found at <http://ncnr.nist.gov/equipment/he3nsf/index.html>.
- <sup>24</sup>Q. Ye *et al.*, *Phys. Procedia* **42**, 206 (2013).
- <sup>25</sup>T. R. Gentile *et al.*, *Physica B* **356**, 96 (2005).
- <sup>26</sup>B. L. Volodin, S. V. Dolgy, E. D. Melnik, E. Downs, J. Shaw, and V. S. Ban, *Opt. Lett.* **29**, 1891 (2004).
- <sup>27</sup>C. Moser and G. Steckman, *Photon. Spectra* **36** (6), 82 (2005).
- <sup>28</sup>P. Nikolaou, N. Whiting, N. A. Eschmann, K. E. Chaffee, B. M. Goodson, and M. J. Barlow, *J. Magn. Reson.* **197**, 249 (2009).
- <sup>29</sup>J. Singh *et al.*, *AIP Conf. Proc.* **1148**, 823 (2009).
- <sup>30</sup>nLIGHT Corporation, 5408 NE 88th Street, Vancouver, WA 98665.
- <sup>31</sup>S. Boag *et al.*, *Physica B* **404**, 2659 (2009).
- <sup>32</sup>OptiGrate Corporation, 3267 Progress Drive, Orlando, FL 32826.
- <sup>33</sup>M. S. Dewey *et al.*, *Nucl. Instrum. Methods Phys. Res. B* **241**, 213 (2005).
- <sup>34</sup>J. A. Dura *et al.*, *Rev. Sci. Instrum.* **77**, 074301 (2006).
- <sup>35</sup>J. W. Lynn *et al.*, *J. Res. Natl. Inst. Stand. Technol.* **117**, 61 (2012).
- <sup>36</sup>C. J. Gilinka *et al.*, *J. Appl. Crystallogr.* **31**, 430 (1998).
- <sup>37</sup>E. Babcock *et al.*, *Phys. Rev. Lett.* **91**, 123003 (2003).
- <sup>38</sup>In some cases, the  $T_1$  listed may not agree with those reported elsewhere. SEOP cells can display a dependence of  $T_1$  on the sign, magnitude and history of the magnetic field (see R. E. Jacob *et al.*, *Phys. Rev. A* **69**, 021401(R) (2004)). When available, here we report the  $T_1$  observed immediately after cooling the cell, with no change in orientation.
- <sup>39</sup>W. G. Williams, *Polarized Neutrons* (Oxford, New York, 1988).
- <sup>40</sup>B. Lancor, Ph.D. dissertation, University of Wisconsin, Madison, Wisconsin, USA, 2011.
- <sup>41</sup>E. Babcock, Ph.D. dissertation, University of Wisconsin, Madison, Wisconsin, USA, 2005.
- <sup>42</sup>B. Lancor, E. Babcock, R. Wyllie, and T. G. Walker, *Phys. Rev. A* **82**, 043435 (2010).
- <sup>43</sup>B. Lancor and T. G. Walker, *Phys. Rev. A* **83**, 065401 (2011).
- <sup>44</sup>B. Lancor and T. G. Walker, *Phys. Rev. A* **82**, 043417 (2010).
- <sup>45</sup>B. Larson, O. Hausser, P. P. J. Delheij, D. M. Whittal, and D. Thiessen, *Phys. Rev. A* **44**, 3108 (1991).
- <sup>46</sup>B. V. Zhdanov and R. J. Knize, *Opt. Eng.* **52**, 021010 (2013).